

## MOLECULAR BIOLOGY OF PHARMACOLOGIC VITREOLYSIS

BY J. Sebag MD, FRCOphth

### ABSTRACT

**Purpose:** Pharmacologic vitreolysis is a promising new therapy to improve vitreoretinal surgery and, ultimately, prevent disease by mitigating the contribution of vitreous to retinopathy. The mechanism of action of the agents being developed for pharmacologic vitreolysis remains unclear. The experiments in this thesis test the hypothesis that pharmacologic vitreolysis agents break down vitreous macromolecules into smaller particles.

**Methods:** Microplasmin, hyaluronidase, and collagenase were tested in solutions of hyaluronan (n = 15) and collagen (n = 15), explants of bovine vitreous (n = 15), dissected porcine vitreous (n = 9), and intact porcine eyes (n = 18). There were also 21 controls, totaling 93 specimens. Vitreous macromolecule sizes were determined with dynamic light scattering (DLS), performed at intervals from 10 minutes to 24 hours following injections.

**Results:** Studies of DLS reproducibility showed a coefficient of variance of less than 3.3% in all but one specimen. Microplasmin decreased porcine vitreous macromolecule size in a dose-dependent manner (correlation coefficient  $r = 0.93$ ), with an 85% reduction after a 30-minute exposure to the maximum dose. Hyaluronidase decreased vitreous macromolecule size in hyaluronan solutions by 50% at high (1,000 IU/mL,  $P < .001$ ) doses and in bovine vitreous by 20%. Collagenase decreased macromolecule size in collagen solutions by 20% at both low (1 mg/mL,  $P < .001$ ) and high (10 mg/mL,  $P < .001$ ) doses, but not at all in bovine vitreous.

**Conclusions:** Pharmacologic vitreolysis can induce a significant decrease in vitreous macromolecule sizes, depending upon the pharmacologic agents and the experimental model. Broad-spectrum agents were more effective than substrate-specific enzymes. Defining the molecular biology of pharmacologic vitreolysis has implications for surgical developments and may impact upon the design of clinical trials to induce prophylactic posterior vitreous detachment.

*Trans Am Ophthalmol Soc 2005;103:473-494*

### INTRODUCTION

Invisible *by design* (Figure 1), vitreous was long *unseen* as important in ocular physiology<sup>1</sup> and as a cause of retinal pathology. In recent years the importance of vitreous in the pathogenesis of various retinopathies has been increasingly appreciated, and vitreous is being treated with ever-evolving therapeutic modalities, for the most part surgical. The future, however, will see an increase in the use of pharmacologic agents for therapy and prevention. Such pharmacologic therapies rely upon a good understanding

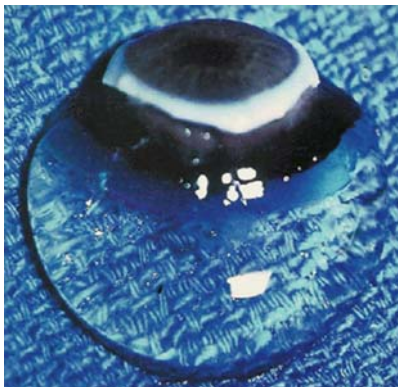


**FIGURE 1**

Human vitreous. Specimen from a 9-month-old child with the sclera, choroid, and retina dissected off the vitreous body. In spite of this specimen being on a surgical towel exposed to room air, the gel state is maintained.

From the VMR Institute, Huntington Beach, California, and the University of Southern California, Los Angeles. The author has been a consultant to ISTA Pharmaceuticals and coinvestigator in the Phase II and Phase III US Food and Drug Administration (FDA) clinical trials of Vitrase; a consultant to ThromboGenics, Ltd; and coinvestigator in the Phase I FDA trial of chondroitinase, funded by Storz.

of the biochemical composition and organization of vitreous, how this structure changes with age, and how anomalies in “normal” aging and systemic diseases lead to vitreoretinal disorders. It is now known<sup>2</sup> that although seemingly clear, the adult human vitreous contains fine, parallel fibers coursing in an anteroposterior direction (Figure 2). Ultrastructural studies<sup>3</sup> have demonstrated that collagen fibrils are the only microscopic structures that correspond to these macroscopic fibers. Furthermore, the chemical interaction of these fibrils with other molecular components of vitreous is now better understood, enabling the development of a

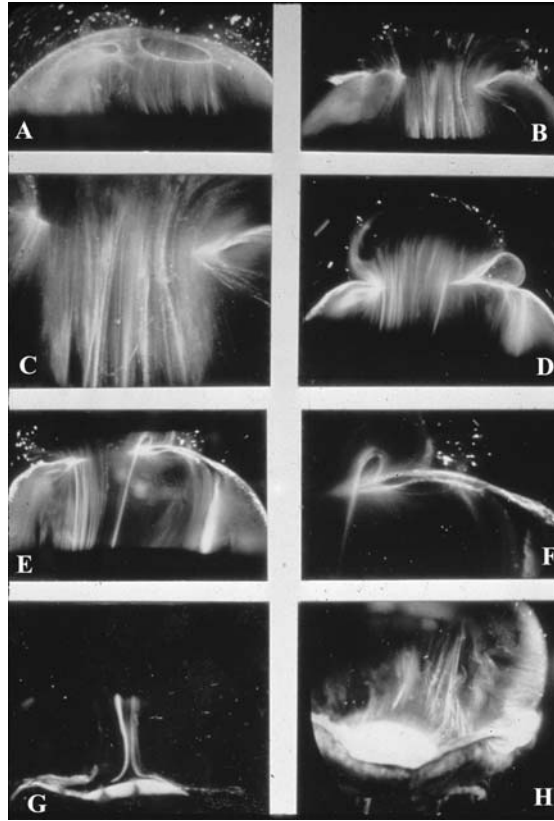


**FIGURE 2**

Dark-field slit microscopy of human vitreous. Sclera, choroid, and retina were dissected off the vitreous body. The specimens are illuminated from the side with a slit-lamp beam and photographed from above at a 90° angle to the plane of illumination, maximizing the Tyndall effect and creating a horizontal optical section through the vitreous body. The anterior segment is below and the posterior pole is above in all photographs. Fibers are seen coursing from the vitreous base (H) to the posterior vitreous (A through D), where they insert into the posterior vitreous cortex (E and F). These fibers form when hyaluronan (HA) molecules dissociate from their molecular association with collagen, the exact nature of which remains to be identified, and no longer separate microscopic collagen fibrils, resulting in cross-linking by adjacent collagen fibrils and the formation of macroscopic vitreous fibers from which HA molecules are excluded. Eventually, the aggregates of collagen attain sufficiently large proportions to be visualized in vitro (Figure 2) and at times clinically. The areas adjacent to these large fibers have a low density of collagen fibrils and a relatively high concentration of HA molecules that scatter much less light than collagen.

pharmacologic approach to treating vitreoretinal disorders, known as pharmacologic vitreolysis. In recent years, pharmacologic vitreolysis has emerged as a new treatment modality to potentially eliminate untoward effects of vitreous upon the retina. Although several agents have been investigated in animal models, only a few have been employed in humans. Autologous plasmin enzyme (APE) has been used in some patients but has never been subjected to the rigors of a controlled clinical trial. Chondroitinase and hyaluronidase have been tested in clinical trials. The former never entered Phase II testing, and hyaluronidase recently failed a Phase III US Food and Drug Administration (FDA) trial conducted in the United States. These disappointing results are due, at least in part, to an insufficient understanding of the molecular effects of the agents being developed for pharmacologic vitreolysis. Thus, the mechanism of action of pharmacologic vitreolysis agents needs to be more clearly defined on a molecular level. This will improve the results of clinical trials and facilitate the development of successful agents.

One fundamental question of scientific interest and clinical relevance is whether or not pharmacologic vitreolysis enzymes break down vitreous macromolecules. The investigations described herein attempt to answer that question by testing the hypothesis that pharmacologic vitreolysis agents do indeed degrade vitreous macromolecules into smaller particles. This hypothesis was tested in model solutions of vitreous biochemistry *in vitro* and postmortem animal models, using noninvasive dynamic light scattering (DLS) to measure vitreous macromolecule diffusion coefficients repeatedly during the experiments and determine vitreous macromolecule sizes before, during, and after treatment. The rationale for using DLS in these investigations relates to the fact that vitreous macromolecules are suspended in solution within the vitreous, and thus if pharmacologic vitreolysis breaks down these macromolecules into smaller particles, there should be an increase in the Brownian movement by the smaller particles. DLS can detect these changes without introducing artifact and thereby prove the hypothesis that pharmacologic vitreolysis induces vitreous macromolecule breakdown.

## VITREOUS BIOCHEMISTRY

That vitreous is now considered an important ocular structure with respect to both normal physiology<sup>4</sup> and several important pathologic conditions of the posterior segment<sup>5</sup> is due in no small part to a better understanding of the biochemical composition and organization of vitreous. Vitreous biochemistry has been extensively reviewed elsewhere.<sup>6-8</sup> The features of vitreous biochemistry that are most relevant to this thesis concern the macromolecules hyaluronan and collagen, because these are the major constituents of vitreous along with water.

### Hyaluronan

Hyaluronan is a major macromolecule of vitreous. Although it is present throughout the body, hyaluronan was first isolated from bovine vitreous in 1934 by Meyer and Palmer. Hyaluronan is a long, unbranched polymer of repeating disaccharide (glucuronic acid  $\beta$  (1,3)-*N*-acetylglucosamine) moieties linked by  $\beta$  1–4 bonds.<sup>9</sup> It is a linear, left-handed, threefold helix with a rise per disaccharide on the helix axis of 0.98 nm.<sup>10</sup> The sodium salt of hyaluronan has a molecular weight of 3 to  $4.5 \times 10^6$  in normal human vitreous.<sup>11</sup> Hyaluronan is not normally a free polymer *in vivo*, but it is covalently linked to a protein core, the ensemble called a proteoglycan.

### Collagen

Recent studies<sup>8</sup> of pepsinized forms of collagen confirmed that vitreous contains collagen type II, a hybrid of types V/XI, and type IX collagen in a molar ratio of 75:10:15, respectively. In the entire body, only cartilage has as high a proportion of type II collagen as vitreous, explaining why certain inborn errors of type II collagen metabolism affect vitreous as well as joints. Vitreous collagens are organized into fibrils (Figure 3) with type V/XI residing in the core, type II collagen surrounding the core, and type IX collagen on the surface of the fibril. The fibrils are 7 to 28 nm in diameter,<sup>12</sup> but their length *in situ* is unknown.

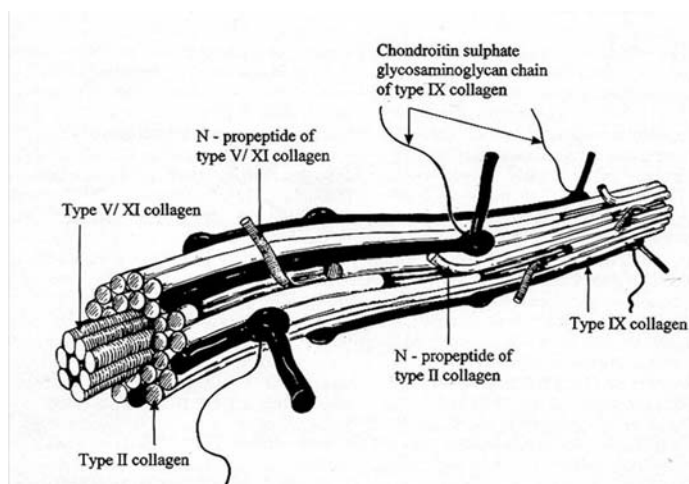


FIGURE 3

Schematic diagram of vitreous collagen fibril structure. This demonstrates the presence of type V/XI in the center, type II collagen surrounding the central core, and type IX collagen on the surface of the fibril.

### Supramolecular Organization

As originally proposed by Balazs and more recently described with precision by Mayne,<sup>13</sup> vitreous is a dilute meshwork of collagen fibrils interspersed with extensive arrays of hyaluronan molecules. The collagen fibrils provide a scaffold-like structure that is “inflated” by the hydrophilic hyaluronan. If collagen is removed, the remaining hyaluronan forms a viscous solution; if hyaluronan is

removed, the gel shrinks<sup>14</sup> but is not destroyed. Comper and Laurent<sup>14</sup> proposed that electrostatic binding occurs between the negatively charged hyaluronan and the positively charged collagen in vitreous.

Bishop<sup>8</sup> has proposed that to appreciate how vitreous gel is organized and stabilized requires an understanding of what prevents collagen fibrils from aggregating and by what means the collagen fibrils are connected to maintain a stable gel structure. Studies<sup>15</sup> have shown that the chondroitin sulfate chains of type IX collagen bridge between adjacent collagen fibrils in a ladder-like configuration spacing them apart. Such spacing is necessary for vitreous transparency, because keeping vitreous collagen fibrils separated by at least one wavelength of incident light minimizes light scattering, allowing the unhindered transmission of light to the retina for photoreception. Bishop proposed that the leucine-rich repeat protein opticin is the predominant structural protein responsible for short-range spacing of collagen fibrils. Concerning long-range spacing, Scott and associates<sup>15</sup> and Mayne and colleagues<sup>16</sup> have claimed that hyaluronan plays a pivotal role in stabilizing the vitreous gel.

#### AGE-RELATED VITREOUS DEGENERATION

During aging, substantial alterations take place in the vitreous body. Beginning after the fourth decade of life, there is a significant decrease in the gel volume and an increase in the liquid volume of human vitreous. Postmortem studies<sup>3,5-7</sup> led to the concept that derangement of the normal hyaluronan/collagen association results in the simultaneous formation of liquid vitreous and aggregation of collagen fibrils into bundles of parallel fibrils seen macroscopically as large fibers (Figure 2). In the posterior vitreous, such age-related changes form large pockets of liquid vitreous, recognized clinically as "lacunae" (Figure 4, bottom right, asterisk). By the ages of 80 to 90 years, more than half the vitreous body is liquid.

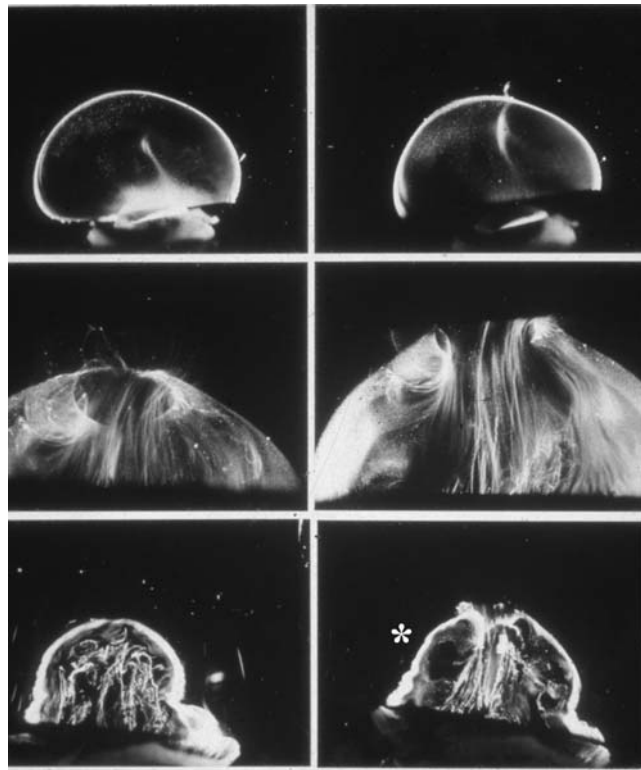


**FIGURE 4**

Age-related changes in human vitreous structure. Top panel: Dark-field slit microscopy of the posterior and central vitreous in a 33-week-old human embryo shows considerable light scattering arising from the peripheral vitreous cortex, due to densely packed collagen fibrils. In the central vitreous is the remnant of the hyaloid artery oriented toward the prepapillary posterior vitreous cortex. This structure is destined to become Cloquet's canal. Middle panel: Vitreous structure in adults is characterized by macroscopic fibers with an anteroposterior orientation, inserting into the vitreous base. Bottom panel: In old age there is aggregation of the fibers into tortuous structures with adjacent pockets of liquid vitreous that form lacunae (asterisk).

During youth, there is strong adhesion between the posterior vitreous cortex and the internal limiting lamina (ILL) of the retina, primarily at the vitreous base and at the posterior pole. Vitreoretinal adhesion at the posterior pole appears to be more fascial<sup>17</sup> than focal (at the disc, fovea, and along retinal blood vessels), consistent with the concept that the two tissues are held together by an extracellular matrix "glue." With age, there is weakening of vitreoretinal adhesion, most likely due to biochemical alterations in the extracellular matrix "glue" at the vitreoretinal interface. Studies using lectin probes<sup>18</sup> have identified that one component of the

extracellular matrix at the vitreoretinal interface [galactose  $\beta$  (1,3)-*N*-acetylglucosamine] is present in youth but absent in adults. This difference and others may play a role in the observed weakening of the vitreoretinal interface during aging. Identifying the nature of these “adhesive” molecules may also provide opportunities for pharmacologic lysis of vitreoretinal adhesion.

## POSTERIOR VITREOUS DETACHMENT

Posterior vitreous detachment (PVD) results from weakening of the adhesion between the posterior vitreous cortex and the ILL, in conjunction with liquefaction within the vitreous body. Weakening of the posterior vitreous cortex/ILL adhesion at the posterior pole allows liquid vitreous to enter the retrocortical space via the prepapillary hole and perhaps the premacular vitreous cortex as well (Figure 2A and Figure 4). Volume displacement from the central vitreous to the preretinal space causes the observed collapse of the vitreous body.

For PVD to occur without complications, two different processes must occur concurrently and to a similar extent: weakening of vitreoretinal adhesion and vitreous liquefaction. There must be sufficient weakening of vitreoretinal adherence so that when the critical amount of liquefied gel has accumulated, the collapsing vitreous separates away from the retina and PVD occurs without untoward effects.

## ANOMALOUS PVD

Anomalous PVD results when the extent of vitreous liquefaction exceeds the degree of vitreoretinal interface weakening, resulting in traction exerted at the vitreoretinal interface.<sup>19</sup> There can be various untoward effects of anomalous PVD. Effects upon the retina include hemorrhage, retinal tears and detachment, vitreomacular traction syndromes, and some cases of diffuse diabetic macular edema. Proliferative diabetic retinopathy can be greatly aggravated by anomalous PVD. Effects upon vitreous involve posterior vitreoschisis,<sup>20</sup> where splitting of the posterior vitreous cortex and forward displacement of the vitreous body leave the outer layer of the split posterior vitreous cortex still attached to the retina. This can result in macular pucker, contribute to macular holes, or complicate proliferative diabetic retinopathy.<sup>19,20</sup>

It is a premise of this thesis that we now understand enough about vitreous biochemistry, structure, and pathology, as related to anomalous PVD, to develop new strategies for treatment and prevention. These emerging new drug therapies will initially enhance surgery but may ultimately replace it as a means of treating and preventing various vitreoretinopathies.

## PHARMACOLOGIC VITREOLYSIS

Pharmacologic vitreolysis is an emerging therapeutic modality intended to mitigate anomalous PVD by chemically altering vitreous structure and weakening vitreoretinal adhesion to safely detach the posterior vitreous. Not only would this facilitate surgery, but it may prevent disease if performed early in the natural history. Various pharmacologic vitreolysis agents have been tested to date,<sup>21-29</sup> but little is known about the exact mechanism of action of these substances, and so far none has met with sufficient success to result in widespread use. Plasmin has been used only in limited series of uncontrolled clinical testing (two published series of nine and seven cases), chondroitinase was used only on 20 patients in a Phase I FDA trial, and hyaluronidase has recently failed a Phase III FDA trial. Without a proper understanding of the molecular effects and the mechanism(s) of action, there could be much wasted research and development with agents that are ultimately ineffective in the clinical setting, as may have been the case with hyaluronidase.

The scientific investigations reported for the first time in this thesis were undertaken to elucidate the mechanism of action of pharmacologic vitreolysis. Specifically, it was hypothesized that pharmacologic vitreolysis agents would break down vitreous macromolecules into smaller particles. This hypothesis was tested using three different enzymes: a broad-spectrum nonspecific protease (human recombinant microplasmin), and two substrate-specific enzymes that specifically target the major macromolecules in vitreous (hyaluronidase and collagenase). These agents were tested in four different experimental models: solutions that model vitreous biochemistry, explants of whole bovine vitreous, dissected porcine vitreous, and intact pig eyes, *postmortem*. Previous studies<sup>5-10,12,13,16</sup> have shown that these species have vitreous that is biochemically similar to human vitreous. A powerful, noninvasive, laser-based technology (DLS) was used to measure vitreous diffusion coefficients and calculate the sizes of the particles in the specimens. In these studies, the average size and the distributions of particle sizes were used as outcome measures of the molecular effects of pharmacologic vitreolysis. A total of 93 experimental and control specimens were studied with the objective to determine whether these enzymes altered vitreous molecular structure, specifically by decreasing the sizes of vitreous macromolecules.

## METHODS

---

### EXPERIMENTAL ENZYMES

#### Microplasmin

Previous studies<sup>22,23,26,27</sup> have suggested that plasmin from a variety of sources may be useful for pharmacologic vitreolysis. APE was reported to induce vitreoretinal separation in rabbits, but there were no studies on the molecular effects of APE. These laboratory investigations were followed by treatment in small series of patients undergoing vitrectomy for macular holes ( $n = 9$ ) and diabetic retinopathy ( $n = 7$ ).<sup>30,31</sup> However, to date, no controlled clinical trials have been undertaken with APE. The methods employed to extract APE from the patient's blood preoperatively have inherent variability, making dosing and quality control difficult. Human recombinant microplasmin, which is much smaller than plasmin and is manufactured in a standardized manner that provides quality control and standardized dosing, is being developed for pharmacologic vitreolysis. Recent studies found that microplasmin is able to

detach the posterior vitreous cortex in pigs<sup>32</sup> and cats and postmortem human eyes.<sup>33</sup> However, as in the case of APE, there are no studies on the molecular effects of microplasmin upon the gel vitreous.

Microplasmin is a direct-acting thrombolytic agent that contains the protease domain but lacks the five “kringle” domains of plasmin, making it a much smaller (molecular weight = 29,000 kDa) molecule than plasmin.<sup>34</sup> The microplasmin (provided by ThromboGenics, Ltd, Dublin, Ireland) used in these experiments was produced with the use of the *Pichia Pastoris* yeast expression system of human microplasminogen. The product was purified, converted to microplasmin with staphylokinase, and equilibrated with 5 mM citrate. In these investigations, microplasmin was diluted with BSS Plus (Alcon, Fort Worth, Texas) and added to the dissected porcine eyes at doses of 0.0125 mg, 0.08 mg, 0.125 mg ( $n = 2$ ), 0.4 mg, and 0.6 mg ( $n = 2$ ), with one placebo specimen. In intact porcine eyes, microplasmin was injected at doses of 0.0125 mg ( $n = 3$ ), 0.125 mg ( $n = 3$ ), 0.25 mg ( $n = 3$ ), 0.5 mg ( $n = 3$ ), and 0.8 mg. Controls were either untreated ( $n = 2$ ) or placebos receiving vehicle injection without the microplasmin enzyme ( $n = 3$ ).

### **Hyaluronidase**

Hyaluronidase is a naturally occurring enzyme that digests proteoglycans, primarily hyaluronan. Purified ovine hyaluronidase (provided by Dr Hampar Karageozian, ISTA Pharmaceuticals, Irvine, California) was diluted with phosphate-buffered saline (PBS) and added to the model vitreous solutions of hyaluronan (0.1 mg/mL) at concentrations of 100 IU/mL ( $n = 5$ ) and 1,000 IU/mL ( $n = 5$ ). This was the same drug as that used in the recent FDA clinical trials in the United States.

In explants of bovine vitreous, hyaluronidase was added at a concentration of 1,000 IU/mL ( $n = 5$ ), and PBS was used as a control solution ( $n = 5$ ). It was hoped that studying the molecular biology of hyaluronidase action in these experiments could shed some light on the negative results obtained in the recent Phase III FDA clinical trial.

### **Collagenase**

Collagenases comprise a group of enzymes that degrade collagen. Just as there are as many as 18 different types of collagen, there are many subtypes of collagenase. Because of the predominance of type II collagen in vitreous, type II-S collagenase (Sigma C1764, St Louis, Missouri) was added to collagen solutions (0.1 mg/mL) at a concentration of 1 mg/mL ( $n = 5$ ) and 10 mg/mL ( $n = 5$ ). In explants of bovine vitreous, collagenase was added at a concentration of 10 mg/mL ( $n = 5$ ), and PBS was used as a control solution ( $n = 5$ ).

## **DYNAMIC LIGHT SCATTERING**

DLS is an established laboratory technique to measure the average size or distribution of sizes of microscopic particles in the range of 3 nm to 3  $\mu\text{m}$  in diameter.<sup>35</sup> Light scattered by a laser beam passing through a dispersion of particles in a solution undergoing random Brownian motion will have intensity fluctuations in proportion to the Brownian motion of the particles. Because the size of the particles influences their Brownian motion, analysis of the scattered light intensity yields a distribution of the size(s) of the suspended particles. The theoretical basis for this methodology and all relevant formulas are presented in Appendix A.

The DLS apparatus (Figure 5) used in these studies was originally developed to conduct fluid physics experiments.<sup>35</sup> It has also been used in research on board the National Aeronautics and Space Administration space shuttle and orbiting space station. Ansari<sup>36</sup> recently authored a comprehensive overview of ophthalmic applications of DLS. These studies and others demonstrated the sensitivity and accuracy of this technology in evaluating lens<sup>37,38</sup> and vitreous<sup>39,40</sup> macromolecules. To perform DLS studies in vitreous, the laser is focused into the specimen, and back-scattered light from a 50 $\mu\text{m}^3$  volume of vitreous is captured by the probe. The detected signal is processed via a digital correlator to yield a time correlation function (TCF; see appendix A for definition, Figure 6 for example). In DLS of vitreous, what is being measured is the diffusion coefficient of the vitreous macromolecules collagen and hyaluronan, for those are the large particles in suspension whose movement influences the characteristics of the back-scattered light. Larger particles, such as collagen, move more slowly than smaller, more flexible particles, such as hyaluronan. Using the formulas described in Appendix A, the measurement of diffusion coefficient can be used to calculate the hydrodynamic radius of the particles (equation 4, Appendix A). Both the diffusion coefficient and the particle size determinations are valid outcome measures when DLS is used for quantitative assessments of vitreous macromolecules. For these studies of the effect of pharmacologic vitreolysis on vitreous macromolecules, 20-nm polystyrene beads (also called *nanospheres*; Bangs Laboratories, Fishers, Indiana) were added so as to provide an easily identifiable internal standard whose signal is unmistakable. Figure 6 compares the TCF of whole porcine vitreous to a solution of 20-nm polystyrene nanospheres.

Previous studies<sup>39,40</sup> have determined that in bovine, porcine, and human eyes, the TCF of vitreous contains two components: (1) the left-most portion of the TCF curve (red in Figure 6), the so-called early or fast component, which corresponds to the hyaluronan macromolecules, and (2) the right-most portion of the curve, the so-called late or slow component, which corresponds to collagen. The findings in Figure 6 are typical of those seen for all untreated control specimens in the studies reported herein and are consistent with previous DLS findings in bovine<sup>39</sup> and human<sup>40</sup> vitreous. The bovine studies showed that DLS is able to measure the size of vitreous macromolecules through the cornea and lens, making it potentially useful in clinical applications. Indeed, studies<sup>37,38</sup> with 267 patients at the National Eye Institute have demonstrated clinical accuracy, reliability, and safety. In the experiments herein, the anterior segment was dissected so as to enable the determination of the best measurement locations in the vitreous body.

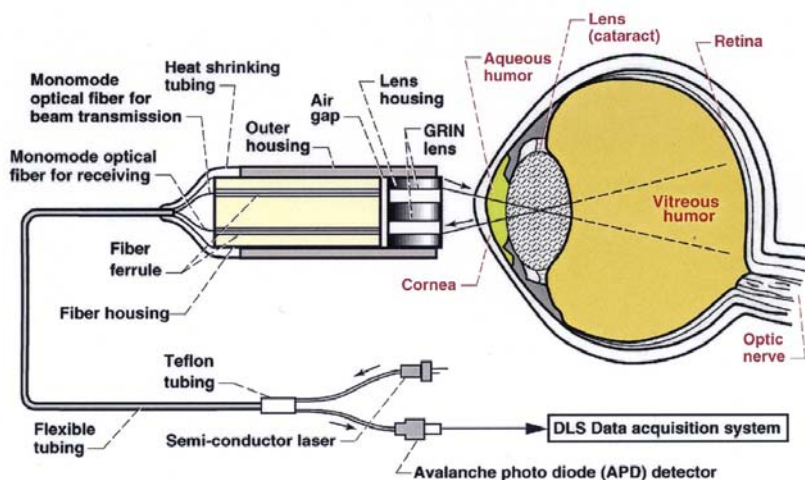


FIGURE 5

Dynamic light-scattering (DLS) apparatus. The main components are a compact fiber optic probe, a computer (Gateway PC 500S) containing a digital correlator card (BI-9000 Brookhaven Instruments, New York), a 635-nm-wavelength 1-mW solid-state laser (OZ Optics, Canada), and an avalanche photo diode detector (Perkin Elmer, Canada). The fiber optic probe is mounted on an optical assembly connected through translational stages controlled manually to access and direct the probe to a desired location in the eye. The DLS probe is composed of two GRIN lenses and two monomode optical fibers, each housed in a stainless steel ferrule, mounted into a separate stainless steel housing. An air gap is intentionally left between the fiber housing and the lens housing in order to produce a tightly focused spot in the test specimen.

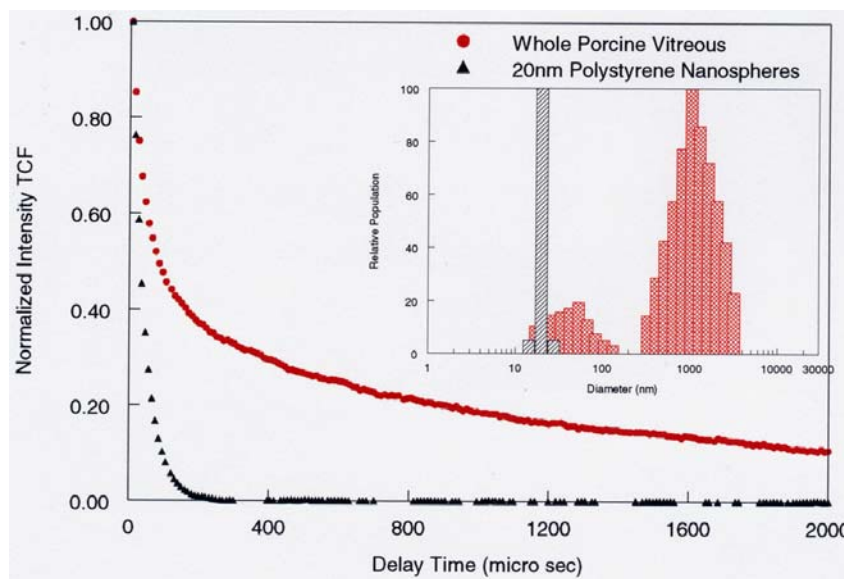


FIGURE 6

Time correlation function (TCF) of whole porcine vitreous. For dilute dispersions of particles, the slope of the TCF provides an accurate determination of the particle's translation diffusion coefficient, which is related to its size (see Stokes-Einstein equation (4), Appendix A). Compared to a solution of 20-nm polystyrene beads (black curve), porcine vitreous has two components to the TCF (red curve), indicating polydispersity. The solution of nanospheres has only one component (monodisperse) that is very fast because of the small size and perfectly spherical shape of the beads, enabling very rapid Brownian movements in the solution. The histograms in the inset display the particle size distributions of these DLS measurements. The group of bars around 1,000 nm diameter correspond to the larger, stiffer (and thus slower moving or diffusing) collagen macromolecules, whereas those around 80 to 100 nm correspond to the smaller, more flexible (and thus faster moving or diffusing) hyaluronan macromolecules. The black bar indicates the 20-nm polystyrene beads, for reference.

## VITREOUS SPECIMENS

### Model Solutions of Vitreous Biochemistry

Vitreous biochemistry was modeled by preparing solutions of the major macromolecules hyaluronan and collagen for *in vitro* study. Hyaluronan is the same in all parts of the body and in all species as well; thus any source provides a good biochemical model for human vitreous hyaluronan. Cartilage collagen is very similar to vitreous, owing to a high concentration of type II collagen, and there are no species variations.

Stock solutions of hyaluronan (TRI-K Industries, Northvale, New Jersey) ( $n = 20$ ) and collagen (Bovine Tracheal Cartilage Type II; Sigma C1188, St Louis, Missouri) ( $n = 20$ ) were diluted to a concentration of 0.1 mg/mL using double-distilled water and then filtered via a 0.22- $\mu$ m filter (Millipore, Bedford, Massachusetts) to remove impurities. These model solutions of vitreous biochemistry were placed into optical cuvettes, experimental enzymes or PBS control solutions were added, and the specimens were incubated at 37°C for 24 hours, with the cuvettes covered to prevent evaporation. At various time points, DLS measurements were performed on these specimens by positioning the DLS probe to the side of the optical cuvettes and focusing the laser into the center of the cuvette.

### Bovine Vitreous Explants *In Vitro*

Bovine eyes ( $n = 15$ ; five treated with hyaluronidase, five treated with collagenase, and five treated with PBS as controls) were obtained from a local abattoir and studied within 3 to 6 hours, during which time they were maintained fresh (unfixed) at 4°C. Because of the relatively large volume of bovine vitreous, only explants of whole gel vitreous were studied *in vitro*. To do so, the anterior segment was excised via a pars planar incision, and 2 mL of gel vitreous was removed and placed into an optical cuvette. Experimental and control solutions were added to the specimens in the cuvettes, which were then kept in an incubator at 37°C for 24 hours, during which time the cuvettes were covered to prevent evaporation. At 2, 4, 6, 12, and 24 hours, the cuvettes were removed from incubation, and DLS measurements were obtained by positioning the DLS probe to the side of the optical cuvettes and focusing the laser into the center of the cuvette.

### Dissected Porcine Vitreous

Pig eyes were obtained from a local abattoir and studied within 3 to 6 hours, during which time they were maintained fresh (unfixed) at 4°C. In nine pig eyes, the anterior segment was excised via a pars planar incision, and control as well as experimental solutions were placed onto the anterior vitreous cortex with the eye in the upright (“supine”) position. DLS measurements were obtained from the central vitreous at a point located 1 mm ( $n = 5$ ) and 4 mm ( $n = 4$ ) behind the anterior vitreous cortex by positioning the DLS probe over the anterior vitreous cortex, focusing the focal point of the DLS laser probe onto the vitreous, identifying the air/vitreous interface by light-scattering criteria, and using the micropositioning control to precisely position the focal point of the DLS laser probe either 1 or 4 mm into the anterior vitreous.

### Intact Pig Eyes

In 18 intact pig eyes, the experimental and control solutions (described above) were injected into the vitreous body with a 30-gauge needle inserted via the pars plana. The eyes were immersed in a water bath at 37°C but shielded from direct contact with the water so as to prevent artifacts. After 30 minutes of incubation, the anterior segment was excised by means of a pars planar incision. With the eyes upright (“supine” position), the DLS probe was positioned over the anterior vitreous cortex and the air/vitreous interface was identified by light scattering criteria. DLS measurements were obtained from multiple points (mean = 18.6, SD = 11.8) along the optical axis extending from the air/vitreous interface to the vitreoretinal interface. The micropositioning control was also used to position the focal point of the DLS laser probe at a depth of 4 mm behind the air/vitreous interface, and DLS measurements were obtained at multiple points (mean = 30.8 points, SD = 18.0) along the horizontal axis from one side of the eye to the other.

## STATISTICAL ANALYSES

Coefficients of variance were calculated to determine the reproducibility of the DLS measurements in model solutions of vitreous as well as explants of whole bovine vitreous.

Pearson’s correlation coefficient ( $r$ ) was used to evaluate the dose-response relation in intact porcine eyes injected with various doses of microplasmin.

Two-way repeated-measures analysis of variance (ANOVA) was used to compare differences in explants of whole bovine vitreous and model solutions of hyaluronan and collagen. Differences were considered significant when the probability value indicated a chance occurrence of less than 5%.

## RESULTS

### REPRODUCIBILITY STUDIES

The reproducibility of DLS measurements was tested to evaluate the reliability of this technique for quantifying vitreous macromolecule sizes in these studies. Ten consecutive DLS measurements were made in optical cuvettes containing untreated explants of whole bovine vitreous ( $n = 3$ ), model solutions of hyaluronan ( $n = 3$ ), and model solutions of collagen ( $n = 3$ ). Table shows that the coefficients of variance were less than or equal to 3.3% in eight of nine groups of specimens and only 8.7% in the ninth group (“Vit 1” in Table). Thus, DLS measurements of vitreous and model solutions of vitreous macromolecules appear to be highly reproducible using this instrumentation and the formulas in Appendix A.

**TABLE. REPRODUCIBILITY OF DYNAMIC LIGHT-SCATTERING (DLS) MEASUREMENTS\***

HA 1	HA 2	HA 3	COLL 1	COLL 2	COLL 3	VIT 1	VIT 2	VIT 3
1.13	1.12	1.10	1.56	1.67	1.55	1.47	1.30	1.43
1.12	1.14	1.11	1.58	1.65	1.67	1.44	1.30	1.41
1.12	1.13	1.13	1.64	1.64	1.56	1.49	1.31	1.39
1.11	1.16	1.09	1.58	1.64	1.66	1.40	1.34	1.39
1.14	1.17	1.15	1.70	1.64	1.58	1.17	1.31	1.37
1.11	1.13	1.11	1.65	1.59	1.60	1.23	1.30	1.37
1.13	1.16	1.11	1.55	1.56	1.57	1.21	1.33	1.39
1.12	1.12	1.11	1.58	1.60	1.58	1.29	1.28	1.32
1.13	1.15	1.11	1.58	1.58	1.70	1.27	1.28	1.45
1.13	1.12	1.16	1.60	1.66	1.56	1.28	1.26	1.39
<b>0.90</b>	<b>1.70</b>	<b>2.00</b>	<b>2.90</b>	<b>2.30</b>	<b>3.30</b>	<b>8.70</b>	<b>1.80</b>	<b>2.50</b>

\*Using DLS, the diffusion coefficient was measured for each of the three samples of hyaluronan (HA 1, 2, and 3), three samples of collagen (Coll 1, 2, and 3), and three explants of whole bovine vitreous (Vit 1, 2, and 3). The bottom row (in bold type) represents the coefficients of variance (%) for the 10 measurements in each specimen.

## MICROPLASMIN

Three separate sets of experiments were conducted to answer the question, “Does microplasmin decrease the size of porcine vitreous macromolecules?”

- The first set of studies employed dissected pig eyes to determine if there was any effect at all by microplasmin on the size of porcine vitreous macromolecules and the approximate time course of these effects.
- The second set of experiments employed dissected pig eyes to determine whether reliable data could be obtained from a location in the anterior vitreous that closely approximates the site of a trans pars plana injection (ie, 4 mm behind the lens).
- The third set of experiments used intact pig eyes to determine if the effects of microplasmin on vitreous macromolecules were dose-dependent.

The following describes the detailed results of these three sets of experiments.

### Microplasmin Effects on Dissected Porcine Vitreous: Determining a Pharmacologic Effect and Its Time Course

In five pig eyes the anterior segment was dissected off the vitreous body by means of a limbal incision. With the eyes oriented in the “supine” position, 0.3 mL of placebo (vehicle) solution or microplasmin at different doses (0.08 mg, 0.125 mg, 0.4 mg, and 0.6 mg) was placed onto the exposed anterior vitreous cortex. The DLS probe was positioned over the anterior vitreous, and measurements were made at a point in the central vitreous located 1 mm behind the anterior vitreous cortex. Measurements were obtained every 10 minutes for up to 6 hours. The results (Figure 7) showed no effects at the lower doses (0.08 mg and 0.125 mg) but significant reduction in the average vitreous macromolecule size at the higher doses (0.4 mg and 0.6 mg). The observed effects began 30 to 90 minutes after introducing the enzyme and reached maximal levels of particle size reduction at 60 to 150 minutes. On the basis of these results, 90 minutes was selected as the optimal time period for the next set of studies in dissected porcine vitreous. Interestingly, the effect with 0.4 mg had a more rapid onset than 0.6 mg, but by 150 minutes the two doses had equivalent effects. This seemingly contradictory finding may be due to the fact that the measurement site was only 1 mm into the anterior vitreous. At this level, dehydration effects during the 6-hour experiment could have introduced artifacts upon the anterior vitreous. Thus, a 4-mm depth was selected as the measurement site for subsequent experiments. It is important to recall that the first set of studies was only intended to determine if there was any measurable effect by microplasmin on vitreous at all and define its time course. With this experimental design and the limited number of samples, no reliable dose-response data can be derived. Indeed, subsequent experiments were designed to do this.

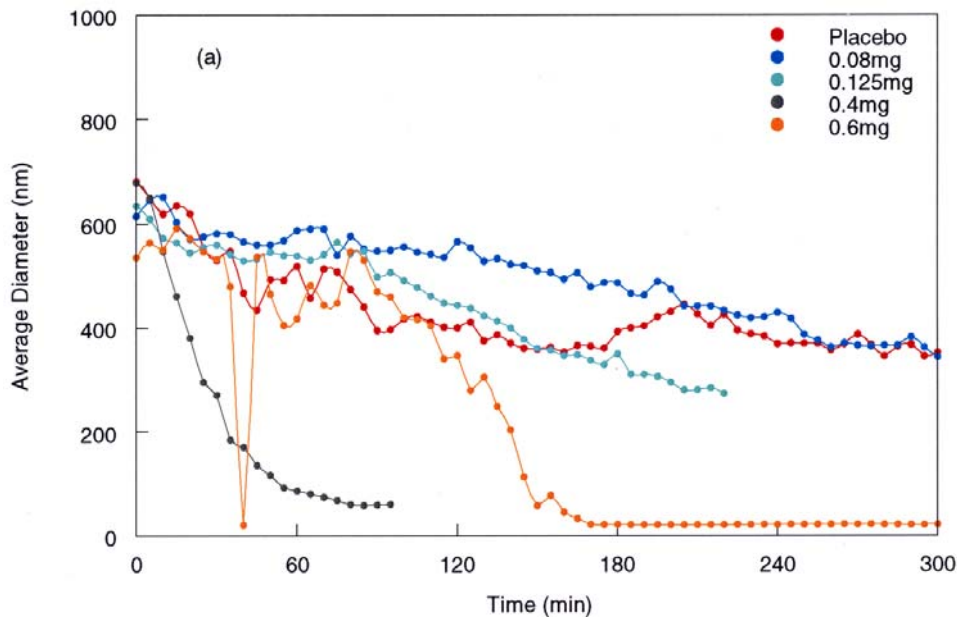


**FIGURE 7**

Effects of microplasmin on vitreous macromolecule sizes in the anterior vitreous of dissected pig eyes. In five pig eyes, the anterior segment was dissected off the vitreous body and microplasmin solutions were placed onto the anterior vitreous cortex. Dynamic light-scattering measurements were made in the central vitreous 1 mm behind the anterior vitreous cortex, and particle sizes were calculated. Measurements were performed frequently (each dot represents one measurement) to define the time course of the phenomenon.

#### Microplasmin Effects on Dissected Porcine Vitreous: Measurement Site Evaluation

Figure 8 shows the DLS findings in four pig eyes following dissection of the anterior segment off the vitreous body by means of a pars planar incision. After 90 minutes of microplasmin pharmacologic vitreolysis, DLS measurements were obtained from a point 4 mm behind the lens and compared to a solution of 20-nm polystyrene beads. The TCF curves (see Appendix A) demonstrate that with increasing doses of microplasmin, there is a decrease in the slope of the TCF curve (shift to the left), signifying a decrease in the sizes of vitreous macromolecules. Eventually, with the highest dose (0.6 mg), the curve approaches the shape of the TCF of the control solution (20-nm polystyrene beads [black triangles] in Figures 6 and 8), meaning that the population of particles consists mostly of smaller-sized molecular species. Because of the reliable uniformity of these results, the measurement site at 4 mm behind the lens was selected as the measurement site for subsequent experiments so as to eliminate some of the artifact detected at the 1-mm measurement site (Figure 8).

#### Microplasmin Effects in Intact Pig Eyes: Dose-Response Studies

Various doses of microplasmin (0.0125mg, 0.125 mg, 0.25 mg, 0.5 mg, and 0.8 mg) and placebo solutions were injected into intact pig eyes ( $n = 18$ ) that were then incubated for 30 minutes at 37°C. After dissecting off the anterior segment, multiple DLS measurements were performed along the optical axis (mean = 18.6, SD = 11.8) and at multiple points (mean = 30.8 points, SD = 18.0) along a horizontal axis in the central vitreous 4 mm behind the anterior vitreous cortex. All measurements (approximately 50 for each eye) were averaged into a single index of the normalized average diameter (see Appendix A) of the vitreous macromolecules in that eye. The results from one run are presented in Figure 9. With increasing doses of microplasmin, there is a shift to the left in the particle size distributions. This is identified by detecting a diminution in the large particle sizes (represented by the bars on the right of the graphs) and an increase in the smaller particle sizes (located to the left). Whereas controls (Figure 9, a and b) and low-dose specimens (Figure 9, c and d) have a considerable representation of macromolecules in the 1,000-nm range, with the 0.5-mg (Figure 9f) and 0.8-mg (Figure 9g) doses there are no longer any particles at all in the 1,000-nm-diameter range.

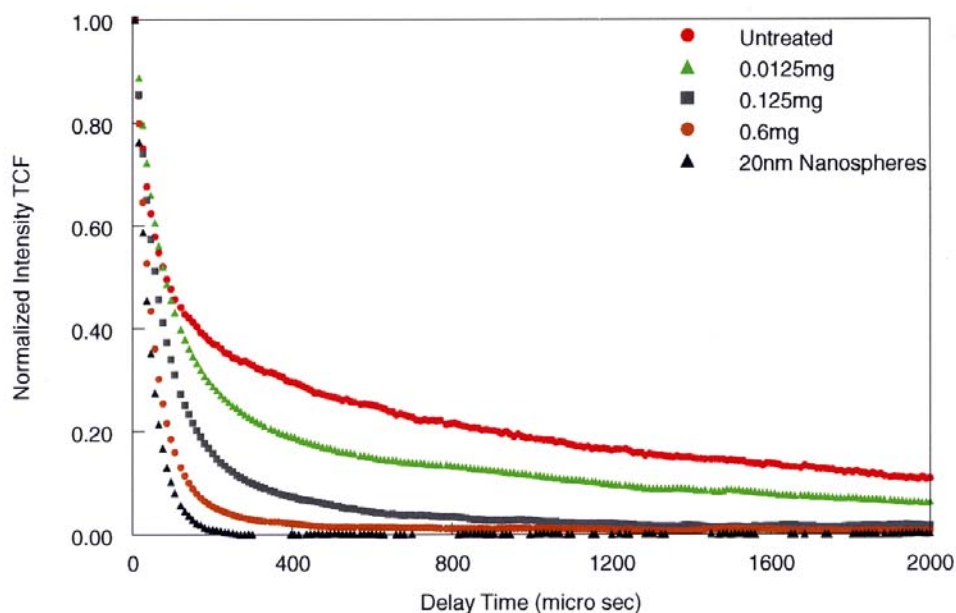


**FIGURE 8**

Dynamic light-scattering (DLS) measurements in porcine vitreous 90 minutes after microplasmin injection 4 mm posterior to the lens. The effects of microplasmin on porcine vitreous are compared to untreated vitreous and a solution of 20-nm polystyrene beads. DLS measurements were performed at a site 4 mm posterior to the anterior vitreous cortex, simulating the intended site of intravitreal injections in vivo. The time correlation function (TCF) curve (see Appendix A) for untreated whole vitreous (red circles) demonstrates the two components previously identified as arising from the major macromolecules hyaluronan and collagen (Figure 6). With increasing doses of microplasmin, there is a decrease in the slope of the TCF, signifying breakdown of the larger vitreous macromolecules, most likely collagen, followed by disappearance of the smaller, more flexible macromolecules, most likely hyaluronan, ultimately approaching the TCF of a pure solution of nanospheres (black triangles.) The smaller particles are likely the breakdown products of the larger vitreous macromolecules induced by microplasmin.

Figure 10 demonstrates the results obtained across the entire range of microplasmin doses in all intact pig eye specimens ( $n = 18$ ). As compared to untreated and vehicle controls ( $n = 5$ ), eyes with microplasmin injection had a significant reduction in vitreous macromolecule sizes. This effect was strongly dose-dependent, as the correlation coefficient across the range of microplasmin doses was considerable ( $r = 0.93$ ).

## HYALURONIDASE

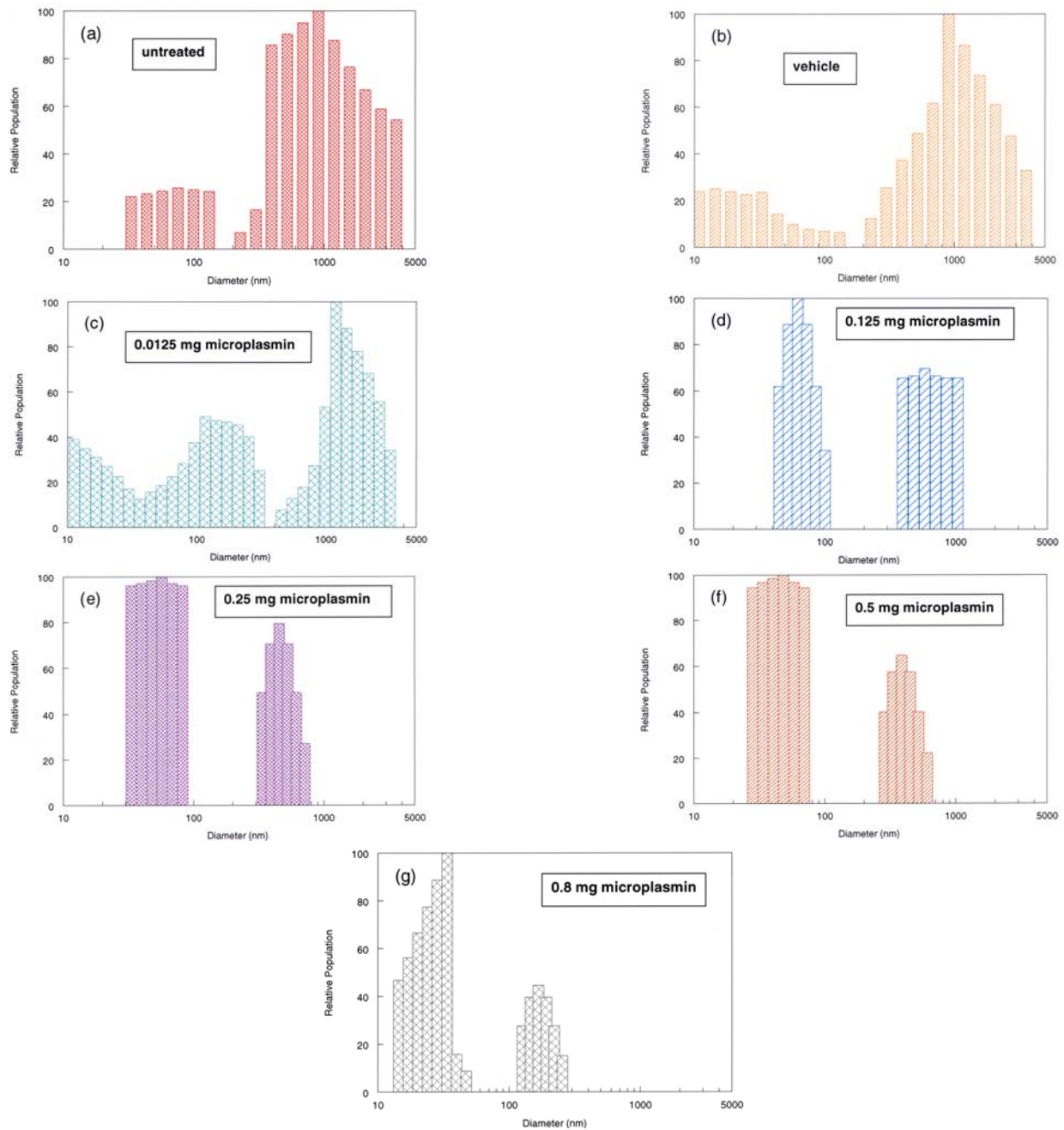
### Molecular Effects of Hyaluronidase on Hyaluronan Solutions

Figure 11 shows the results obtained when a hyaluronan solution was treated with two different doses of hyaluronidase (Figure 11A: low dose of 100 IU/mL,  $n = 5$ ; Figure 11B: high dose of 1,000 IU/mL,  $n = 5$ ). Hyaluronidase decreased macromolecule size in these hyaluronan solutions by about 40% (100 IU/mL,  $P < .001$ ) and 50% (1,000 IU/mL,  $P < .001$ ). This phenomenon manifested after 2 hours and reached a plateau at 6 hours, and these levels were maintained for 24 hours. At each time point after the addition of hyaluronidase, the differences from baseline for each of the concentrations of enzyme were statistically significant ( $P < .001$ ). No significant difference was found between low and high doses of enzymes. In a separate set of experiments (Figure 12), hyaluronidase ( $n = 5$ ) was compared to PBS controls ( $n = 5$ ). The differences between hyaluronidase (100 IU/mL) and PBS controls were significant ( $P = .006$  by ANOVA).

### Molecular Effects of Hyaluronidase on Bovine Vitreous

Explants of whole bovine vitreous were incubated in optical cuvettes with hyaluronidase ( $n = 5$ ). DLS measurements were performed in the optical cuvettes after 2, 4, 6, 12, and 24 hours. The results (Figure 13) showed that after incubating whole bovine vitreous with hyaluronidase (1,000 IU/mL), there was less than a 20% decrease in the average particle size that manifested by 2 hours, reached a steady-state plateau by 6 hours ( $P < .001$ ), but was not sustained at 24 hours, at which point the difference from baseline was no longer statistically significant. This is probably the result of collagen fibril aggregation, because under normal circumstances, hyaluronan intercalates between collagen fibrils and they cannot cross-link, thereby minimizing light scattering and maintaining vitreous

transparency. Degradation of hyaluronan by hyaluronidase exposes collagen fibrils to allow them to cross-link, and by the 24-hour time point in these experiments, an increase in the size of particles is detected by DLS.



**FIGURE 9**

Particle size distribution of porcine vitreous macromolecules following microplasmin pharmacologic vitreolysis. Controls (a = untreated, b = vehicle) and various doses of microplasmin (c = 0.0125 mg, d = 0.125 mg, e = 0.25 mg, f = 0.5 mg, g = 0.8 mg) were injected into intact porcine eyes. After 30 minutes incubation at 37°C, the anterior segment was excised and dynamic light-scattering (DLS) measurements were made at multiple sites along the optical and horizontal axes as described in the “Methods” section. The histograms were derived from the time correlation function (TCF) curves (as shown in Figure 6) and demonstrate the particle size distributions at different doses. Compared with lower doses of microplasmin (c and d), higher doses of microplasmin (f and g) are associated with a shift to left in the particle size distributions, representing a breakdown in vitreous macromolecules. Note that whereas controls (a and b) and low-dose specimens (c and d) have a considerable representation of macromolecules in the 1,000-nm range, at the 0.5-mg (f) and 0.8-mg (g) doses there are no longer any particles in the 1,000-nm range.

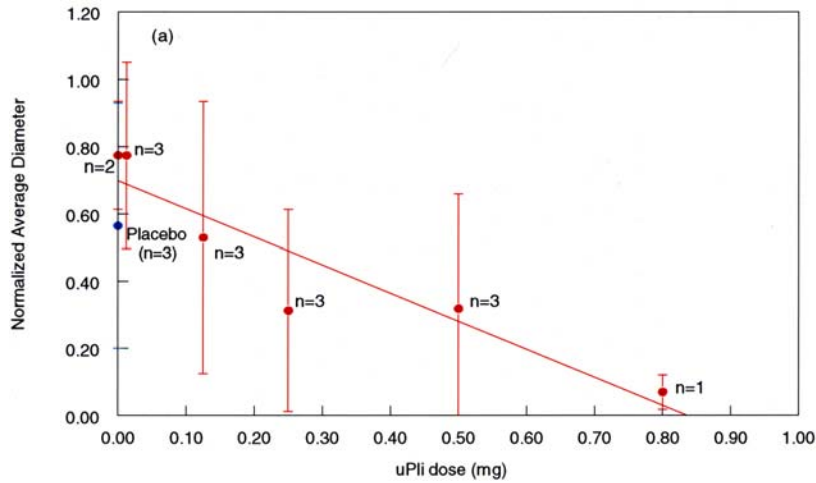


**FIGURE 10**

Microplasmin effects on intact pig eyes. As compared to placebos (blue dot, n = 3) and untreated controls (x-axis value = 0.00, n = 2), there is a considerable reduction in the normalized average diameter of vitreous macromolecules with increasing doses of microplasmin ( $\mu$ Pli). At the maximum dose, there is an 85% reduction in the normalized average diameter of vitreous macromolecules. Error bars indicate the standard deviation of the means

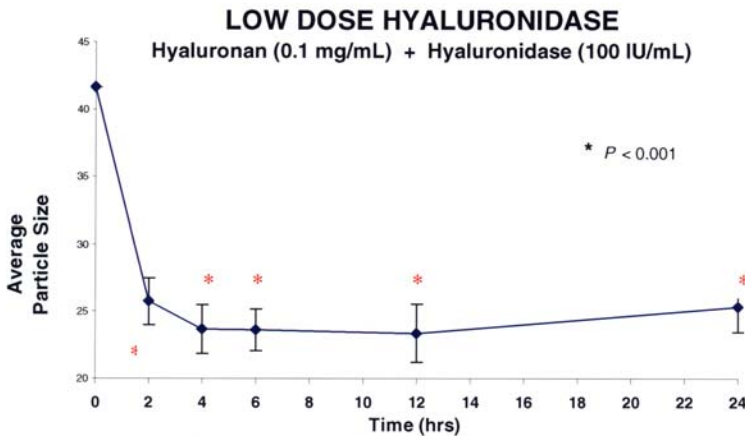


**FIGURE 11A**

Low-dose hyaluronidase effects on model vitreous (hyaluronan) solutions. Each point represents the average of five separate specimens, and the error bars are the standard error of the mean. Statistics compare each point to time zero. The low dose of hyaluronidase employed in this study decreased average particle size (arbitrary units) by about 40%. The effect was apparent at 2 hours and remained statistically significant throughout the study period of 24 hours.

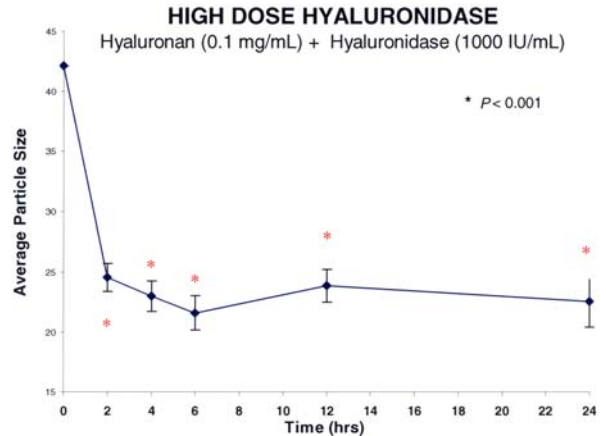


**FIGURE 11B**

High-dose hyaluronidase effects on hyaluronan solutions. Each point represents the average of five separate specimens, and the error bars are the standard error of the mean. The statistical analyses compare each point to time zero, and statistical significance is indicated by the red asterisks. The high dose of hyaluronidase decreased average particle size (arbitrary units) by about 50% ( $P < .001$ ). The effect was apparent at 2 hours and remained statistically significant throughout the study period of 24 hours.

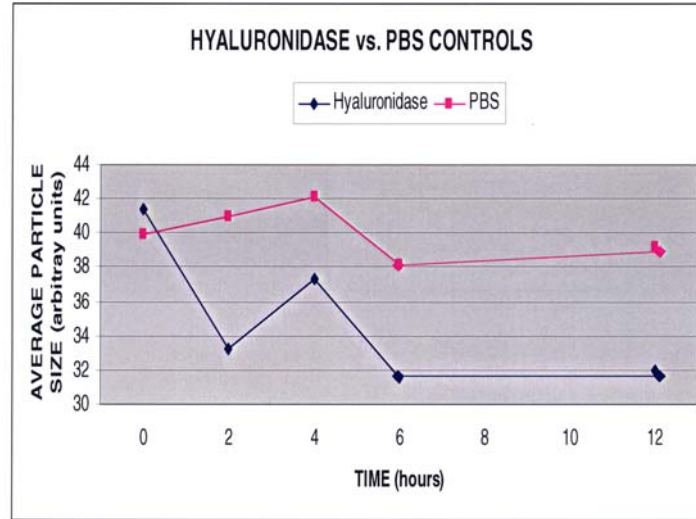


**FIGURE 12**

Hyaluronidase compared to phosphate-buffered saline (PBS) controls in hyaluronan solutions. Each point in the graph represents the average of five separate specimens processed simultaneously. There were significantly ( $P = .006$ ) smaller particle sizes following treatment with hyaluronidase (100 IU/mL) as compared to PBS controls.

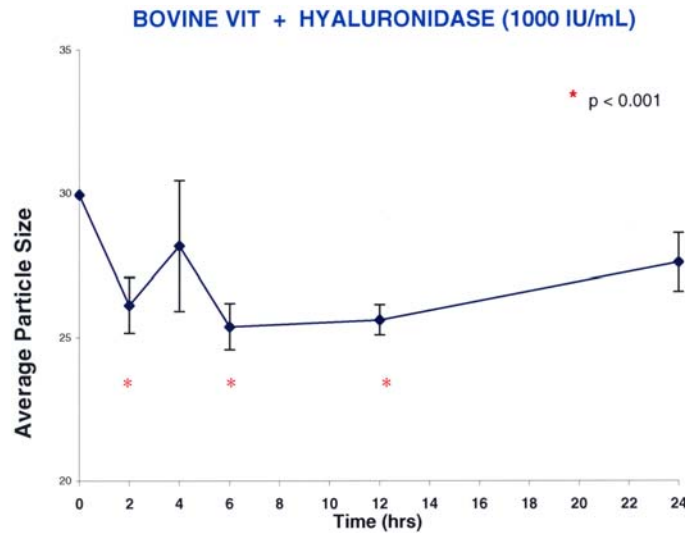


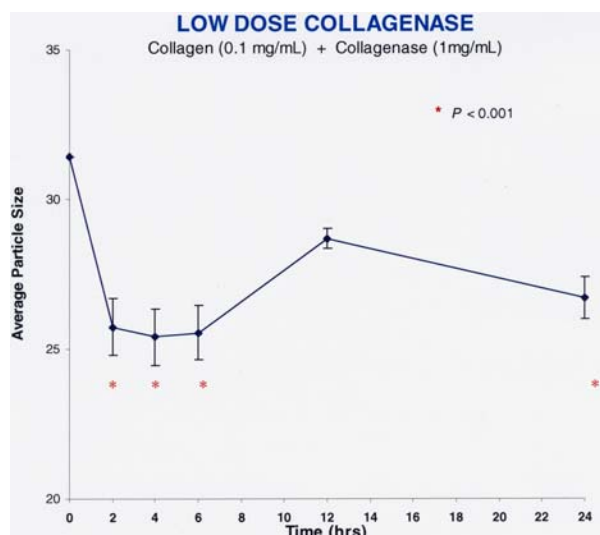
**FIGURE 13**

Hyaluronidase (high-dose) effects on bovine vitreous. Each point represents the average of five specimens run simultaneously, and the error bars signify the standard deviation of the mean. Statistics compare each point to time zero (red asterisk signifies significance). There was less than a 20% decrease in the average particle size (arbitrary units) that manifested by 2 hours and reached a steady-state plateau by 6 to 12 hours ( $P < .001$ ). The effect was not sustained at 24 hours, when the difference from baseline was no longer statistically significant.

## COLLAGENASE

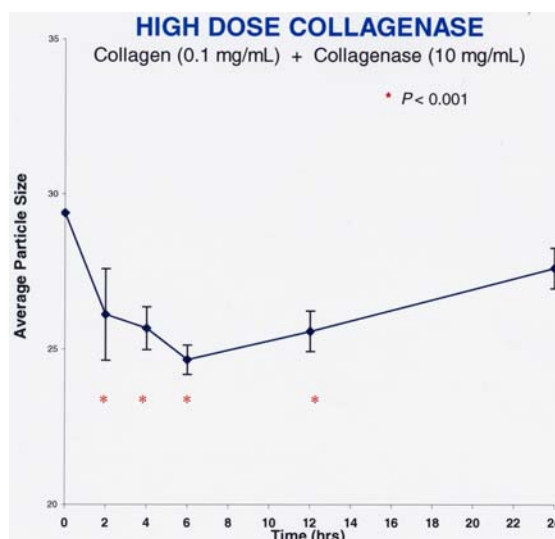
### Molecular Effects of Collagenase on Collagen Solutions

Figure 14 shows the findings after pharmacologic vitreolysis treatment of collagen solutions with collagenase (Figure 14A: low-dose collagenase = 1 mg/mL, n = 5; Figure 14B: high-dose collagenase = 10 mg/mL, n = 5). Collagenase decreased particle sizes by about 20% at both low and high doses ( $P < .001$ ). These effects were apparent at 2 hours after enzyme administration, were sustained at nearly each time point thereafter, and were statistically significant in comparison to baseline.



**FIGURE 14A**

Low-dose collagenase effects on model solutions of collagen. Each data point represents the average of five specimens run simultaneously, and the error bars signify the standard deviation of the mean. Statistics compare each point to time zero, and significance ( $P < .001$ ) is indicated by the red asterisks. Within 2 hours of administration, collagenase decreased vitreous average particle size (arbitrary units) to statistically significant levels, with a maximum effect of a little less than 20%.



**FIGURE 14B**

High-dose collagenase effects on collagen solutions. Each data point represents the average of five specimens run simultaneously, and the error bars signify the standard deviation of the mean with the red asterisks indicating significance. Within 2 hours of administration, high doses (10 mg/mL) of collagenase decreased average particle sizes in collagen solutions (0.1 mg/mL) to statistically significant levels. However, the maximum effect was less than a 20% reduction in average particle size ( $P < .001$ ). There was a substantial increase in macromolecule sizes at 24 hours, perhaps due to cross-linking of digested components of collagen.

### Molecular Effects of Collagenase on Bovine Vitreous

Explants of whole bovine vitreous were treated with collagenase (10 mg/mL; n = 5) or PBS controls (n = 5) and incubated at 37°C in optical cuvettes for 24 hours. Measurements were obtained at 0, 2, 4, 6, 12, and 24 hours. As shown in Figure 15, there was an initial decrease in particle sizes with collagenase, although not a statistically significant difference. By 24 hours, there was a significant increase in the particle sizes as compared to baseline. This unexpected finding is likely due to the propensity of collagen fibrils to cross-link, even after partial enzyme degradation. Continued cross-linking during the duration of the experiment likely resulted in the observed increase in particle sizes by the 24-hour time point, as compared to baseline.

The same experiments were performed using PBS as a control solution instead of a pharmacologic vitreolysis enzyme. Figure 16 shows that there were no effects by this control agent. Separate runs of collagenase (1 mg/mL; n = 5) versus PBS controls (n = 5) added to model solutions of collagen showed no differences in diffusion coefficients with the control PBS solution (data not shown). The findings were similar to the results shown in Figure 16.

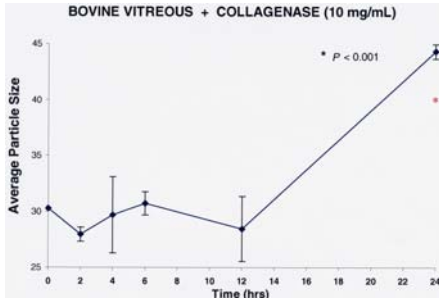


**FIGURE 15**

Collagenase effects on bovine vitreous. Each point represents the average of five separate specimens run simultaneously, and the error bars signify the standard deviation of the mean. Statistics compare each point to time zero, and the red asterisk signifies a significant difference from baseline. At 2 and 12 hours, there was a slight decrease in the average macromolecule sizes, but this was not statistically significant. The substantial (>50 %) increase in particle sizes at 24 hours may be the result of re-aggregation of digested components of collagen, a molecule that has a strong predilection for cross-linking and aggregation.

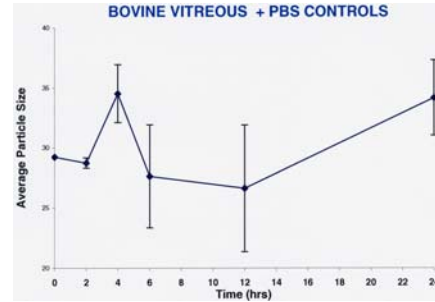


**FIGURE 16**

Controls for pharmacologic vitreolysis of bovine vitreous. Each point represents the average of five separate specimens, and the error bars are the standard error of the mean. There were no statistically significant effects of phosphate-buffered saline (PBS) on macromolecule sizes in bovine vitreous.

## DISCUSSION

PVD results from age-related liquefaction of gel vitreous and concurrent weakening of vitreoretinal adhesion causing collapse of the vitreous body and separation from the retina (Figure 17). During aging, PVD may actually be desirable in the sense that after a certain age, the physiologic role that vitreous played during youth may have lost its importance and the risk that an attached vitreous will exert traction upon the retina becomes more significant. Thus, nature may have evolved a means by which the vitreous separates from the retina later in life. This decreases the chances that untoward effects will be exerted by vitreous upon the retina during aging. In some cases, however, the PVD process is not successful.

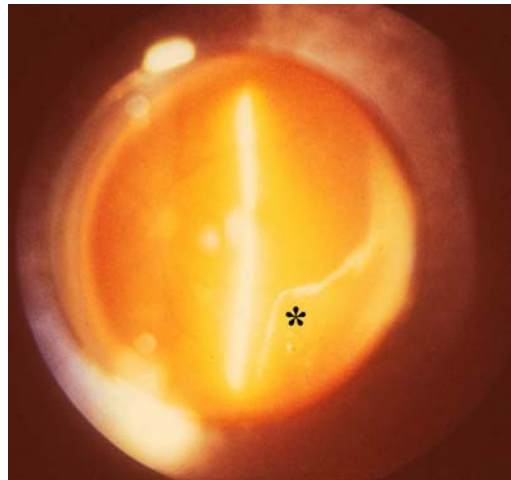


**FIGURE 17**

Posterior vitreous detachment. Vitreous liquefaction (synchysis) in conjunction with dehiscence at the vitreoretinal interface results in liquid vitreous dissecting the posterior vitreous cortex (asterisk) away from the internal limiting lamina of the retina. Collapse (syneresis) of the superior vitreous can be seen in the upper right corner of the photograph.

Anomalous PVD results from vitreous liquefaction without concurrent dehiscence at the vitreoretinal interface. This unifying concept in vitreoretinal diseases proposes that conditions that were previously considered as disparate in etiology are actually quite similar in their mechanisms of disease. Thus, for example, whereas diabetic vitreoretinopathy<sup>41</sup> and myopic vitreoretinopathy<sup>42</sup> are due to different etiologies, the mechanism by which they cause vitreoretinal disease is likely the same. In each condition, there is considerable vitreous liquefaction but insufficient weakening at the vitreoretinal interface to allow for an innocuous PVD, resulting instead in anomalous PVD.

Anomalous PVD is the inciting event in a variety of vitreoretinopathies, such as rhegmatogenous retinal detachment, macular pucker, and macular holes, and a contributing factor in proliferative diabetic retinopathy. Such untoward consequences of anomalous PVD are currently treated surgically to relieve vitreoretinal traction. The future, however, will see less invasive approaches predicated upon the ability of drugs to alter vitreous macromolecules and weaken vitreoretinal adhesion, known as *pharmacologic vitreolysis*.

Pharmacologic vitreolysis<sup>43</sup> is an emerging therapy to treat and prevent anomalous PVD. Successful implementation depends upon a better understanding of the molecular effects of different enzymes so that the most effective ones can be used appropriately in the correct settings. In the case of pharmacologic vitreolysis as an adjunct to vitreoretinal surgery, the ability to lyse vitreous adhesion to the retina is of paramount importance. To enable other clinical applications, pharmacologic vitreolysis agents must also break down vitreous macromolecules. In 25-gauge vitrectomy surgery, for example, it would also be advantageous to pharmacologically break down vitreous macromolecules so as to decrease vitreous macroviscosity and facilitate surgical removal. Such a pharmacologic adjunct would make the surgical approach safer and faster, facilitating this surgery in outpatient and office settings. The breakdown of vitreous macromolecules is also important in pharmacologic vitreolysis induction of prophylactic PVD. In this clinical application, it is also necessary to lyse vitreoretinal adhesion, ideally prior to the onset of macromolecule breakdown and liquefaction, so as to avoid *creating* an anomalous PVD. Prophylactic PVD should be advantageous in patients at risk of developing neovascularization from the optic disc or retina, in high myopia, and in fellow eyes of patients with macular holes and rhegmatogenous retinal detachments, as well as other clinical circumstances. However, to date, there has been little investigation concerning the molecular effects of pharmacologic vitreolysis.

This thesis reports the results of original investigations undertaken to elucidate and quantify the effects of pharmacologic vitreolysis on a molecular level. Three different enzymes (a nonspecific protease; microplasmin; and two substrate-specific enzymes, hyaluronidase and collagenase) were studied in four different experimental systems (model solutions of vitreous biochemistry, explants of whole bovine vitreous, dissected porcine vitreous, and intact pig eyes) employing a total of 93 experimental and control specimens. Although enzymes from different species were employed (eg, ovine hyaluronidase in bovine vitreous), these studies were in vitro and thus an immune response was not a factor. The objective was to determine whether these enzymes decreased the sizes of vitreous macromolecules. A powerful, laser-based technology (DLS)<sup>35-40</sup> was used to determine whether pharmacologic vitreolysis decreased the sizes of vitreous macromolecules. The results of these studies showed that in nearly all instances there was a reduction in the size of vitreous macromolecules. There were, however, some interesting differences between the different enzymes.

Microplasmin induced a dose-dependent reduction in porcine vitreous macromolecule size in both dissected porcine vitreous specimens and intact pig eyes, the latter with a correlation coefficient of 0.93. At the highest dose there was an overall reduction of about 85% after just 30 minutes. This time frame seems acceptable in terms of the amount of time that would be desirable for pharmacologic vitreolysis to have a clinical effect, especially in the operating room as an adjunct to surgery. In terms of inducing prophylactic PVD, studies in pigs, cats, and postmortem human eyes<sup>32,33</sup> suggest that microplasmin can detach the posterior vitreous from the retina. Thus, the new findings reported herein, showing that microplasmin substantially reduces vitreous macromolecule size, suggest that this agent can induce both components of PVD (ie, gel liquefaction and vitreoretinal dehiscence). Microplasmin may therefore be effective in inducing a prophylactic PVD, thereby preventing anomalous PVD and its untoward sequelae.<sup>19</sup> Indeed, broad-acting agents, such as microplasmin, may have a higher likelihood of inducing both a breakdown in vitreous macromolecules and vitreoretinal separation. However, there may also be untoward side effects if the agent's action is too broad. Dispase is an interesting case in point. Although two pig studies<sup>24,28</sup> initially showed efficacy and safety, the results of a more extensive recent study<sup>29</sup> in rabbit and human eyes found that dispase caused retinal toxicity, perhaps due to the broad range of proteins subject to its enzyme action. Thus, rather than employing a single broad-acting substance such as microplasmin or dispase, a combination of highly specific agents, such as collagenase, hyaluronidase, or chondroitinase, may be safer and more effective.<sup>44</sup> The potential need for substrate-specific pharmacologic vitreolysis enzymes led to the investigations reported in this thesis using enzymes with specificity for the major macromolecules of vitreous hyaluronan and collagen.

Hyaluronidase decreased macromolecule sizes in model solutions of vitreous hyaluronan and whole bovine vitreous. Although effective in hyaluronan solutions, hyaluronidase achieved less than a 20% reduction in particle sizes in whole bovine vitreous, likely due to the presence of other macromolecules such as collagen and chondroitin sulfate in whole vitreous. Thus, at this dose range, the effects of hyaluronidase were not as prominent as those observed with the nonspecific protease microplasmin. This is perhaps due to a difference in dosing but may also relate to the fact that if hyaluronidase were truly substrate-specific, it would probably not degrade collagen and the other molecular components of vitreous, whereas the nonspecific nature of microplasmin would enable it to have effects on all proteinaceous molecules in vitreous. Thus, in this instance, a broad-acting agent may be more effective than a substrate-specific agent. This might explain why recent studies<sup>45</sup> found that plasmin was able to induce PVD, whereas hyaluronidase was not effective, confirming previous findings.<sup>46</sup> Moreover, the limited action of hyaluronidase in whole vitreous on a molecular level and the lack of a sustained effect on whole vitreous past 12 hours may explain the relative lack of efficacy that was observed in recent FDA clinical trials of hyaluronidase in clearing vitreous hemorrhage. Thus, further research would seem to be appropriate before

widespread use of hyaluronidase in drug therapy of the posterior segment.

Of the three pharmacologic vitreolysis agents tested in these studies, collagenase had the least effect. In solutions composed of collagen from bovine articular cartilage, type II-S collagenase decreased particle sizes by less than 20% at both low (1 mg/mL,  $P < .001$ ) and high (10 mg/mL,  $P < .001$ ) doses. There were slight effects on explants of whole bovine vitreous at 2 hours, and indeed an increase in particle size was observed after 4 and 6 hours of exposure that was significant at 24 hours. It is hypothesized that this is due to cross-linking of partially digested collagen fibrils and would suggest that if this agent were used as a surgical adjunct, surgery should be performed within 2 hours of drug injection. It is plausible that the minimal effects of collagenase in model solutions of vitreous biochemistry and whole vitreous are due to the use of low doses. Future studies should attempt to use higher enzyme concentrations. Another consideration is that because vitreous collagen fibrils are composed of several collagen subtypes in a unique structural arrangement (Figure 3), any pharmacologic vitreolysis agent(s) intended to break down this vitreous macromolecule must be effective upon all the collagen subtypes in order to access the innermost molecules. It is possible that the lack of significant effects of collagenase in these studies relates to the inability of the type II-S collagenase enzyme that was employed to digest the type V/XI hybrid and type IX collagen present in vitreous. Thus, although type II is the predominant collagen type in vitreous, it is not known whether the type II collagenase used in these studies was able to access the type II collagen surrounding the core of the vitreous collagen fibril (see Figure 3). If future studies determine that drug delivery is impaired at the local level by "other" collagens, then it might be necessary to devise ways to take apart the collagen fibril so as to enable enzyme access to its substrate. A third possible explanation for these findings is that there actually was an enzymatic effect, but that it was not detected by DLS. Recent studies<sup>47,48</sup> have shown that there can be two mechanisms by which collagenases act upon collagen: a triple helical peptidase activity and a collagenolytic activity. The former unravels the triple helix but does not cut the long strands into smaller pieces. Unraveling collagen without segmenting into smaller pieces of collagen may not be detected by DLS as employed in this study. Thus, future studies should explore by what precise mechanism(s) various collagenases alter vitreous collagen so as to select the most potent enzyme subtypes and determine the best way(s) to detect their effects.

DLS appears to be a very powerful investigational tool. It also has potential to improve clinical evaluation for both research and practice. Throughout the history of medicine, increased knowledge of anatomy, better characterization of pathology, and the elucidation of pathogenesis in molecular terms have enabled the evolution of therapeutics from surgical to medical strategies, and ultimately to preventative modalities. Necessary for this progress are an understanding of the molecular basis of disease and new diagnostic technologies that can detect these molecular changes. DLS may enable ophthalmologists to identify early (molecular) stages of disease, so as to develop less invasive and more potent therapeutic interventions and, ultimately, preventative treatment modalities. Such landmark innovations will allow us to prevent early *physiopathology* from advancing to the more advanced *histopathology* we currently recognize by ophthalmoscopy and biomicroscopy as disease, and thereby enable us to prevent irreversible damage to the eye and deleterious effects upon vision.

## SUMMARY

In the future, vitreous surgery will be enhanced by pharmacologic adjuncts to facilitate vitreoretinal separation and vitreous removal. Eventually, these vitreolytic agents will obviate the need for such surgery by reducing the role of vitreous in retinopathy and thereby prevent disease. Pharmacologic vitreolysis is an emerging form of drug therapy that is based upon recent advances in our understanding of vitreous biochemistry and the role of anomalous PVD in the pathophysiology of vitreoretinopathies. Various pharmacologic agents are in development, but little is known about their mechanism of action on a molecular level.

This thesis describes the results of experiments that tested the hypothesis that pharmacologic vitreolysis enzymes break down vitreous macromolecules into smaller particles. Microplasmin, hyaluronidase, and collagenase were tested on model vitreous solutions, explants of whole bovine vitreous, dissected porcine vitreous, and intact pig eyes. A powerful, noninvasive, laser-based technology called dynamic light scattering was used to measure vitreous diffusion coefficients and calculate particle sizes as an outcome measure of the molecular effects of pharmacologic vitreolysis. A total of 93 experimental and control specimens were studied with the objective to determine whether these enzymes decrease the sizes of vitreous macromolecules.

The results showed that microplasmin decreased porcine vitreous macromolecule size by 85% after 30 minutes, making it a reasonable drug to test in clinical trials. Hyaluronidase was much less effective, with only a 50% reduction of macromolecule size in model solutions of vitreous biochemistry, and less than a 20% reduction in whole bovine vitreous. Collagenase had the least potency, perhaps related to dosing or the lack of enzyme access to the unique assembly of vitreous collagen fibrils.

More extensive *in vitro* testing of these and other agents should be followed by appropriate animal model studies before treating patients. Clinical trials should be designed to prove one or more of these agents safe and effective.<sup>49</sup> Safety should be shown not only for the retina, but for the lens and ciliary body as well. Efficacy should be demonstrated for both the breakdown of vitreous macromolecules and dehiscence at the vitreoretinal interface. In spite of these challenges, progress promises to be rapid because the prospect of reducing or even eliminating the pathology that leads to rhegmatogenous retinal detachments, macular holes, advanced diabetic retinopathy, and other causes of blindness is too compelling for practitioners and patients around the world.

## ACKNOWLEDGMENTS

The author is greatly indebted to Dr Rafat Ansari and Dr Kwang Su of the NASA Glenn Research Center in Cleveland, Ohio, who were collaborators on all aspects of these investigations, and Dr Stephan Dunker of Bonn, Germany, and Dr Norihiko Kitaya of

Asahikawa, Japan, who conducted the experiments during their fellowships at the VMR Institute and the Doheny Eye Institute of the University of Southern California.

## APPENDIX A

### DYNAMIC LIGHT SCATTERING

#### General Theory

The technique of dynamic light scattering (DLS) was originally developed to study dispersions of colloidal ( $\leq 1 \mu\text{m}$  in size) particles in fluid. Light scattered by a laser beam passing through such a dispersion will have intensity fluctuations resulting in a constantly fluctuating speckle pattern.<sup>50</sup> This speckle pattern is the result of interference in the light paths, and it fluctuates as the particles in the scattering medium perform random movements on a time scale of  $\geq 1 \mu\text{sec}$  due to the collisions between themselves and the fluid molecules (Brownian motion). In the absence of particle-particle interactions (dilute dispersions), light scattered from small particles fluctuates rapidly, whereas light scattered from large particles fluctuates more slowly. During a simple homodyne experiment, only scattered light is collected (absence of local oscillator) at a photodetector. Assuming that the particles are uniformly sized and spherically shaped, and an intensity-intensity temporal autocorrelation function (also called time correlation function, or TCF) is measured and defined as

$$g^2(\tau) = A[1 + \beta \exp(-2\Gamma\tau)] = A[1 + |g^1(\tau)|^2] \quad (1)$$

where  $A = \langle i \rangle^2$  is the average DC photocurrent or the baseline of the autocorrelation function, and  $\beta$  ( $0 < \beta < 1$ ) is an empirical experimental constant and is a measure of the spatial coherence of the scattering geometry of the collection optics which can be related to signal-to-noise (S/N). In equation (1),  $\Gamma$  is a decay constant due to diffusing motion of the particles in the scattering volume, and  $\tau$  is the delay time. Thus,

$$\Gamma = D_T \cdot q^2 \quad (2)$$

where  $D_T$  is the translational diffusion coefficient and  $q$  is the magnitude of the scattering wave vector, defined as

$$q = \frac{4\pi n}{\lambda} \sin\left(\frac{\theta}{2}\right) \quad (3)$$

where  $n$  is the refractive index of the solvent,  $\lambda$  is the wavelength of the incident light in a vacuum, and  $\theta$  is the scattering angle. Using the Stokes-Einstein relationship for spherical particles,  $D_T$  can be related to the hydrodynamic radius ( $R$ ) of the particle, as

$$D_T = \frac{KT}{6\pi\eta R} \quad (4)$$

where  $K$  is Boltzmann's constant ( $1.38 \times 10^{-23} \text{ J K}^{-1}$ ),  $T$  is the absolute temperature of the scattering medium, and  $\eta$  is the solvent viscosity. In clinical ophthalmic applications, for  $n$  and  $\eta$ , the value of water can be used at a body temperature of  $37^\circ\text{C}$ . Equation 4 then can be used to determine the average size or distribution of sizes of the particles in any colloidal dispersions, including ocular tissues.

For dilute dispersions of spherical particles the slope of the TCF provides a quick and accurate determination of the particle's translational diffusion coefficient, which can be related to its size via a Stokes-Einstein equation, provided the viscosity of the suspending fluid, its temperature, and its refractive index are known. For the lens and vitreous, a viscosity of  $\eta = 0.8904$  centipoise, a refractive index of  $n = 1.333$ , and a temperature of  $25^\circ\text{C}$  for room temperature studies and  $37^\circ\text{C}$  for body temperature studies were used to determine macromolecule sizes.

#### DLS OF VITREOUS

DLS of vitreous provides dynamic information, such as diffusion coefficient, size, scattered intensity, and polydispersity (measure of heterogeneity). Ansari<sup>36</sup> recently authored a comprehensive overview of ophthalmic applications of DLS and their current state of development. Previous studies determined that with this DLS apparatus, the TCF obtained in bovine<sup>39</sup> and human<sup>40</sup> vitreous exhibits bimodal behavior, consistent with the two-component composition of vitreous, due to the macromolecules hyaluronan and collagen. A breakdown of these components following pharmacologic vitreolysis can lead to a broader size distribution or polydispersity. Monodisperse systems can easily be evaluated by single exponential decay or time constant described in equation 1. For polydisperse systems, equation 1 is rewritten as follows:

$$g^1(\tau) = \int_0^\infty F(\Gamma) \exp(-\Gamma\tau) d\Gamma \quad (5)$$

where  $F(\Gamma)$  is the fraction of the total scattered intensity contributed by the particles with decay rates in the range  $\Gamma$  to  $d\Gamma$ . The  $n$ th central moment of this decay rate distribution is given by

$$\mu_n = \int_0^\infty F(\Gamma)(\Gamma - \langle \Gamma \rangle)^n d\Gamma \tag{6}$$

Where

$$\langle \Gamma \rangle = \int_0^\infty \Gamma F(\Gamma) d\Gamma \tag{7}$$

is the average decay rate. A cumulant expansion of equation 6 yields

$$\ln[g^1(\tau)] = - \langle \Gamma \rangle \tau + (1/2!) \mu_2 \tau^2 - (1/3!) \mu_3 \tau^3 + (1/4!) [\mu_4 - 3\mu_2^2] \tau^4 \dots \tag{8}$$

where the coefficients of the terms in  $\tau, \tau^2, \tau^3, \dots$  are the first, second, and third,  $\dots$  cumulants, respectively. The first moment is the average decay constant  $\Gamma$  from which the translational diffusion coefficient is deduced since  $D_T = q^2 / \Gamma$  (see equation 2).

The polydispersity parameter describing the width of the decay rate distribution is given by

$$PDP \equiv \mu_2 / \langle \Gamma \rangle^2 = \int_0^\infty (\Gamma - \langle \Gamma \rangle)^2 F(\Gamma) d\Gamma / \langle \Gamma \rangle^2 \tag{9}$$

In general, an increase in particle sizes (from nanometers to a few microns) and an increase in the number or density of these particles result in an increase in scattered light intensity. Polydispersity is a measure of the number of distinct groups of species with different size(s). In a DLS measurement, up to three groups differing in size can be identified, because they diffuse at different rates (ie, small particles move faster and large particles move more slowly). Therefore, a change in scattered light intensity and polydispersity can complement the particle size data. The data presented herein were analyzed using the cumulant and exponential size distribution routines obtained from Brookhaven Instruments, New York. These schemes have been reviewed and validated by Stock and Ray.<sup>51</sup>

**APPENDIX B. EXPERIMENTAL AND CONTROL VITREOUS SPECIMENS STUDIED BY DYNAMIC LIGHT SCATTERING BEFORE AND AFTER PHARMACOLOGIC VITREOLYSIS**

ENZYME	SPECIMEN	MODEL	MEASUREMENT SITE	PURPOSE	N	TABLE/FIGURE NO.
	Hyaluronan	Synthetic solution	Optical cuvette	Reproducibility	3	Table
	Collagen	Synthetic solution	Optical cuvette	Reproducibility	3	Table
	Bovine vitreous	Explanted	Optical cuvette	Reproducibility	3	Table
	Nanospheres	Synthetic solution	Optical cuvette	Baseline comparisons	1	Figures 6 and 8
	Porcine vitreous	Explanted	Optical cuvette	Baseline comparisons	1	Figure 6
Microplasmin	Porcine vitreous	Dissected	1 mm into intact vitreous	Pharmacologic vitreolysis	5	Figure 7
Microplasmin	Porcine vitreous	Dissected	4 mm into intact vitreous	Pharmacologic vitreolysis	4	Figure 8
Microplasmin	Porcine vitreous	Intact eye	Along optical axis to retina and along	Pharmacologic vitreolysis	18	Figures 9 and 10
Hyaluronidase	Hyaluronan	Synthetic solution	Optical cuvette	Pharmacologic vitreolysis	10	Figure 11
Hyaluronidase	Hyaluronan	Synthetic solution	Optical cuvette	Control comparison	5	Figure 12
PBS	Hyaluronan	Synthetic solution	Optical cuvette	Control	5	Figure 12
Hyaluronidase	Bovine vitreous	Explanted	Optical cuvette	Pharmacologic vitreolysis	5	Figure 13

**APPENDIX B (CONTINUED). EXPERIMENTAL AND CONTROL VITREOUS SPECIMENS STUDIED BY DYNAMIC LIGHT SCATTERING BEFORE AND AFTER PHARMACOLOGIC VITREOLYSIS**

ENZYME	SPECIMEN	MODEL	MEASUREMENT SITE	PURPOSE	N	TABLE/FIGURE NO.
Collagenase	Collagen	Synthetic solution	Optical cuvette	Pharmacologic vitreolysis	10	Figure 14
Collagenase	Bovine vitreous	Explanted	Optical cuvette	Pharmacologic vitreolysis	5	Figure 15
PBS	Bovine vitreous	Explanted	Optical cuvette	Control	5	Figure 16
Collagenase	Collagen	Synthetic solution	Optical cuvette	Pharmacologic vitreolysis	5	NS
PBS	Collagen	Synthetic solution	Optical cuvette	Control	5	NS
					<b>Total No. of specimens</b>	<b>93</b>

NS = not shown; PBS = phosphate-buffered saline.

## REFERENCES

- Sebag J, Balazs EA. Pathogenesis of C.M.E: anatomic consideration of vitreoretinal adhesions. *Surv Ophthalmol* 1984;28(suppl):493-498.
- Sebag J, Balazs EA. Human vitreous fibres and vitreoretinal disease. *Trans Ophthalmol Soc U K* 1985;104:123-128.
- Sebag J, Balazs EA. Morphology and ultrastructure of human. Vitreous fibers. *Invest Ophthalmol Vis Sci* 1989;30:1867-1871.
- Foulds WS. Is your vitreous really necessary? The role of the vitreous in the eye with particular reference to retinal attachment, detachment and the mode of action of vitreous substitutes. (The 2nd Duke-Elder Lecture). *Eye* 1987;1:641-664.
- Sebag J. *The vitreous: structure, function and pathobiology*. New York: Springer-Verlag; 1989.
- Sebag J. Macromolecular structure of vitreous. *Progr Polym Sci* 1998;23:415-446.
- Sebag J. Vitreous—from biochemistry to clinical relevance. In: Tasman W, Jaeger EA, eds. *Duane's Foundations of Clinical Ophthalmology*. Vol 1, chap 16. Philadelphia: Lippincott Williams & Wilkins; 1998.
- Bishop PN. Structural macromolecules and supramolecular organisation of the vitreous gel. *Prog Ret Eye Res* 2000;19:323-344.
- Balazs EA. Molecular morphology of the vitreous body. In: Smelser GK, ed. *The Structure of the Eye*. New York & London: Academic Press; 1961:293-310.
- Sheehan JK, Atkins EDT, Nieduszynski IA. X-Ray diffraction studies on the connective tissue polysaccharides. Two dimensional packing scheme for threefold hyaluronic chains. *J Mol Biol* 1975;91:153-163.
- Balazs EA. Functional anatomy of the vitreous. In: Duane TD, Jaeger EA, eds. *Biomedical Foundations of Ophthalmology*. Philadelphia: Harper & Row; 1984:14.
- Seery CM, Davison PF. Collagens of the bovine vitreous. *Invest Ophthalmol Vis Sci* 1991;32:1540-1550.
- Mayne R. The eye. In: Royce PM, Steinmann B, eds. *Connective Tissue and Its Heritable Disorders*. New York: Wiley-Liss; 2002:131-141.
- Comper WD, Laurent TC. Physiological functions of connective tissue polysaccharides. *Physiol Rev* 1978;58:255-315.
- Scott JE, Chen Y, Brass A. Secondary and tertiary structures involving chondroitin and chondroitin sulphate in solution, investigated by rotary shadowing electron microscopy and computer simulation. *Eur J Biochem* 1992;209:675-680.
- Mayne R, Brewton RG, Ren Z-H. Vitreous body and zonular apparatus. In: Harding JJ, ed. *Biochemistry of the Eye*. London: Chapman and Hall; 1997:135-143.
- Sebag J. Age-related differences at the human vitreo-retinal interface. *Arch Ophthalmol* 1991;109:966-971.
- Russell SR, Shepherd JD, Hageman GS. Distribution of glycoconjugates in the human internal limiting membrane. *Invest Ophthalmol Vis Sci* 1991;32:1986-1995.
- Sebag J. *Anomalous PVD—a unifying concept in vitreo-retinal disease*. Graefes Arch Clin Exp Ophthalmol 2004;242:690-698.
- Chu T, Lopez PF, Cano MR, et al. Posterior Vitreoschisis—an echographic finding in proliferative diabetic retinopathy. *Ophthalmology* 1996;103:315-322.
- Personal communication. For more information, see: Hageman GS, Russell SR Chondroitinase-mediated disinsertion of the primate vitreous body. *Invest Ophthalmol Vis Sci* 1994; 35(ARVO):1260.

22. Verstraeten T, Chapman C, Hartzler M, et al. Pharmacologic induction of PVD in the rabbit. *Arch Ophthalmol* 1993;111:849-854.
23. Hikichi T, Yanagiya N, Kado M, et al. Posterior vitreous detachment induced by injection of plasmin and sulfur hexafluoride in the rabbit vitreous. *Retina* 1999;19:55-58.
24. Tezel TH, Del Priore LV, Kaplan HJ. Posterior vitreous detachment with dispase. *Retina* 1998;18:7-15.
25. Bishop PN, McLeod D, Reardon A. Effects of hyaluronan lyase, hyaluronidase, and chondroitin ABC lyase on mammalian vitreous gel. *Invest Ophthalmol Vis Sci* 1999;40:2173-2178.
26. Unal M, Peyman GA. The efficacy of plasminogen-urokinase combination in inducing posterior vitreous detachment. *Retina* 2000;20:69-75.
27. Hesse L, Nebeling B, Schroeder B, et al. Induction of posterior vitreous detachment in rabbits by intravitreal injection of tissue plasminogen activator following cryopexy. *Exp Eye Res* 2000;70:31-39.
28. Oliveira LB, Tatebayashi M, Mahmoud TH, et al. Dispase facilitates posterior vitreous detachment during vitrectomy in young pigs. *Retina* 2001;21:324-331.
29. Jorge R, Oyamağucji EK, Cardillo JA, et al. Intravitreal injection of dispase causes retinal hemorrhages in rabbit and human eyes. *Curr Eye Res* 2003;26:107-112.
30. Trese MT, Williams GA, Hartzler MK. A new approach to stage 3 macular holes. *Ophthalmology* 2000;107:1607-1611.
31. Williams JG, Trese MT, Williams GA, et al. Autologous plasmin enzyme in the surgical management of diabetic retinopathy. *Ophthalmology* 2001;108:1902-1905.
32. Valmaggia C, Willekens B, de Smet M. Microplasmin induced vitreolysis in porcine eyes. *Invest Ophthalmol Vis Sci* 2003;44(ARVO):3050.
33. Gandorfer A, Rohleder M, Sethi C, et al. Posterior vitreous detachment induced by microplasmin. *Invest Ophthalmol Vis Sci* 2004;45:641-647.
34. Laroche Y, Collen D. Recombinant human microplasmin: production and potential therapeutic properties. *Thromb Haemost* 2003;1:307-313.
35. Ansari RR, Suh KI, Arabshahi A, et al. A fiber optic probe for monitoring protein aggregation, nucleation and crystallization. *J Crystal Growth* 1996;168:216-226.
36. Ansari RR. Ocular static and dynamic light scattering: a non-invasive diagnostic tool for eye research and clinical practice. *J Biomed Opt* 2004;9:46-57.
37. Datiles MB, Ansari RR, Reed GF. A clinical study of the human lens with a dynamic light scattering device. *Exp Eye Res* 2002;74:93.
38. Datiles MB, Ansari RR. Evaluation of cataracts. In: Tasman W, Jaeger EA, eds. *Duane's Clinical Ophthalmology*. Philadelphia: Lippincott Williams & Wilkins; 2004: chap 73-B.
39. Ansari RR, Dunker S, Suh K, et al. Quantitative molecular characterization of bovine vitreous and lens with non-invasive dynamic light scattering. *Exp Eye Res* 2001;73:859-866.
40. Sebag J, Ansari RR, Dunker S, et al. Dynamic light scattering of diabetic vitreopathy. *Diabetes Technol Ther* 1999;1:169-176.
41. Sebag J. Diabetic vitreopathy. *Ophthalmology* 1996;103:205-206.
42. Sebag J. Myopia effects upon vitreous—significance for retinal detachments. Acta V International Congress on Vitreo-Retinal Surgery (M. Stirpe, ed). New York: Ophthalmic Communications Society Inc; 1998:366-372.
43. Sebag J. Pharmacologic vitreolysis. *Retina* 1998;18:1-3.
44. Sebag J. Is pharmacologic vitreolysis brewing? *Retina* 2002;22:1-3.
45. Wang ZL, Zhang X, Xu X, et al. PVD following plasmin but not hyaluronidase—implications for combination pharmacologic vitreolysis therapy. *Retina* 2005;25:38-43.
46. Hikichi T, Masanori K, Yoshida A. Intravitreal injection of hyaluronidase cannot induce posterior vitreous detachment in the rabbit. *Retina* 2000;20:195-198.
47. Lauer-Fields JL, Fields GB. Triple-helical peptide analysis of collagenolytic protease activity. *Biol Chem* 2002;383:1095-1105.
48. Lauer-Fields JL, Sritharan T, Stack MS, et al. Selective hydrolysis of triple-helical substrates by matrix metalloproteinase-2 and -9. *J Biol Chem* 2003;278:18140-18145.
49. Schachat AP, Chambers W, Liesegang TJ, et al. Safe and effective. *Ophthalmology* 2003;110:2073-2074.
50. Chu B. Laser light scattering: basic principles and practice. New York: Academic Press; 1991.
51. Stock RS, Ray WH. Interpretation of photon correlation data: a comparison of analysis methods. *J Polym Sci* 1985;23:1393-1447.